# Dependence of recombination mechanisms and strength on processing conditions in polymer solar cells

Kanwar S. Nalwa,[1] Hari K. Kodali,[2] Baskar Ganapathysubramanian,[2,a)] and Sumit Chaudhary[1,b)]
[1]*Department of Electrical and Computer Engineering, Iowa State University, Ames, Iowa 50011, USA*
[2]*Department of Mechanical Engineering, Iowa State University, Ames, Iowa 50011, USA*

(Received 12 September 2011; accepted 25 November 2011; published online 27 December 2011)

Charge carrier recombination due to carrier trapping is not often considered in polymer based solar cells, except in those using non-fullerene acceptors or new donor polymers with limited short-range order. However, we show that even for the canonical poly(3-hexylthiophene): phenyl-C61-butyric acid methyl ester (P3HT:PCBM) system, relative strengths of bimolecular and trap-assisted recombination are strongly dependent on processing conditions. For slow-grown active-layers, bimolecular recombination is indeed the major loss mechanism under one sun illumination. However, for fast-grown active-layers, trap-assisted recombination dominates over bimolecular recombination by an order of magnitude, and recombination strength at short-circuit condition is 3-4 times higher, leading to loss of photocurrent and lowering of fill factor. © *2011 American Institute of Physics*. [doi:10.1063/1.3671999]

Solution processed organic photovoltaic (OPV) cells fabricated from blends of conjugated polymers and fullerene derivatives are showing impressive progress, with power conversion efficiencies improving notably in the last decade. Recent improvement in power conversion efficiencies owes to the development of new conjugated polymers[1] and optimizations in materials processing/fabrication conditions.[2–5] Such optimizations include approaches like annealing the active-layer in solvent atmosphere,[2,5,6] thermal annealing, post-production thermal annealing after deposition of metal electrode on the active-layer,[3] and using high-boiling point solvents as additives.[4]

Utilizing annealing in solvent-atmosphere (also called solvent-annealing) to control nanomorphology was one of the key developments for OPVs; Li *et al*. showed that desirable morphology is achieved by slowing the bulk-heterojunction (BHJ) film growth rate, or in other words, by increasing the time it takes for the wet films to solidify.[2] It was shown that slow growth rate leads to a higher order in the $\pi$-conjugated structure of P3HT, enhanced optical absorption with more pronounced vibronic shoulders, and more balanced carrier transport.[2,5] Evidence of de-mixing of PCBM and subsequent stacking of P3HT chains was also shown by Miller *et al*.[6] However, the effect of growth rate on some other crucial device parameters remained unknown. Two such important parameters included defects within the P3HT domains and carrier recombination rate/mechanism. Elucidating the effect of these parameters is important for better understanding of process-structure-property relationships because carrier recombination accounts for more than 30% loss in modern OPV cells,[7] and defects strongly affect carrier recombination dynamics.[8]

In a recent publication,[9] we elucidated the dependence between growth-rate and density of sub-band gap defect states in the P3HT phase of P3HT:PCBM devices. Within the set of devices we investigated, we showed that slower growth rate leads to reduction in the density of sub-band gap defect states by one order of magnitude.[9] We also observed that light intensity dependence of open circuit voltage ($V_{oc}$) is strongly affected by defect states. In this report, we investigate the effect of growth rates on recombination dynamics in P3HT:PCBM based BHJ OPV cells. We couple our experimental results and device parameters with a drift-diffusion based device model and show that under one sun illumination, bimolecular recombination is the major loss mechanism for slow-grown active-layers and exceeds the interfacial trap-assisted recombination loss by an order of magnitude. However, for fast-grown active-layers with high trap density, the trap-assisted recombination dominates over the intrinsic bimolecular recombination by an order of magnitude.

In P3HT:PCBM BHJ solar cells, the recombination of free charge carriers is attributed to bimolecular (Langevin) recombination, the rate of which is given by

$$R_{Bimolecular} = \gamma(np - n_i p_i), \tag{1}$$

where $n$ ($p$) is the free electron (hole) density, $n_i$ ($p_i$) is the intrinsic electron (hole) density, and $\gamma$ is the Langevin recombination constant.[10] Trap-assisted recombination is usually neglected, except for OPVs with non-fullerene acceptors,[11] or donors with limited short-range order.[12] Trap-assisted recombination involves trapping of one type of carrier at defect states within a donor or acceptor phase and its subsequent recombination with free carriers in the other phase. The trap-assisted recombination rate is given by the Shockley-Read-Hall (SRH) equation

$$R_{SRH} = \frac{C_n C_p N_t (pn - p_1 n_1)}{[C_n(n + n_1) + C_p(p + p_1)]}, \tag{2}$$

where $C_n$ and $C_p$ are the capture coefficients of electrons and holes, respectively, $N_t$ is the density of traps, $n$ and $p$ are the

a)Electronic mail: baskarg@iastate.edu.
b)Electronic mail: sumitc@iastate.edu.

 

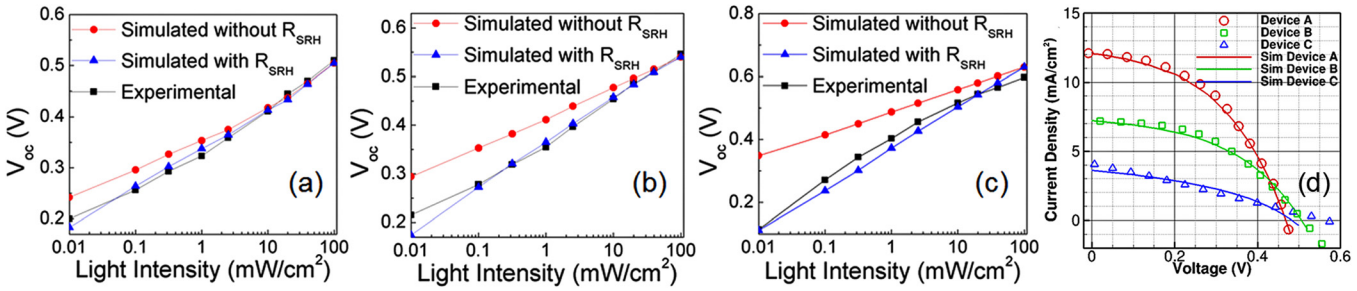


FIG. 1. (Color online) Experimental (squares) $V_{oc}$ versus light intensity of P3HT:PCBM devices (a) A, (b) B, and (c) C; and simulated $V_{oc}$ with (triangle) and without (circle) SRH recombination ($R_{SRH}$). In case of simulations without $R_{SRH}$, only Langevin recombination was used to calculate the *J-V* characteristics with experimentally measured carrier mobilities, an e-h pair distance a = 2 nm, and decay rate $k_f = 1.5 \times 10^2\ s^{-1}$. For calculations with $R_{SRH}$, both SRH and Langevin recombination mechanisms were incorporated in the model, taking into account the trapping parameter (reported in our earlier publication, Ref. 9) $N_t = 3.3 \times 10^{21}\ m^{-3}$, $5.2 \times 10^{21}\ m^{-3}$, and $2.1 \times 10^{22}\ m^{-3}$ for devices A, B, and C, respectively, and the capture coefficients for electrons and holes $C_n = C_p = 6 \times 10^{-16}\ m^3\ s^{-1}$. (d) Measured (open symbols) *J-V* characteristics of P3HT:PCBM OPV devices A, B, and C. The solid lines are the calculated *J-V* characteristics after incorporating SRH recombination, with maximum generation rates $G_{max} = 5 \times 10^{28}\ m^{-3}\ s^{-1}$, $3.5 \times 10^{27}\ m^{-3}\ s^{-1}$, and $8 \times 10^{26}\ m^{-3}\ s^{-1}$ for devices A, B, and C, respectively.

electron density in the conduction band and the hole density in valence band, and $p_1 n_1 = N_c N_v \exp[-(E_c - E_v)/kT] = n_i^2$, with $n_i$ the intrinsic carrier concentration.[8]

To investigate the effect of growth rate on recombination rates/mechanisms, we analyzed three types of P3HT:PCBM BHJ cells—A, B, and C—wherein the active layers were spin coated at 400, 600, and 1000 rpm for 30, 60, and 60 s, obtaining solvent evaporation times of ~40, 7, and 1 min and thicknesses of 350, 220, and 140 nm, respectively. Device fabrication and characterization of these solar cells were presented in our previous report.[9] Characterization included current-voltage characteristics, determination of defect densities using capacitance measurements, and dependence of $V_{oc}$ on light intensity. For this report, in order to simulate the photocurrent and correlate it with defect densities, we used a numerical device model that included drift and diffusion,[13,14] the field- and temperature-dependent generation rate $G(E,T)$, carrier mobilities, and trap densities. The model also included thickness dependence of maximum generation rate $G_{max}$, which is lower for thicker films as it represents an average value over the film thickness. For devices A, B, and C, respectively, total density of hole traps as reported in our previous publication[9] were $3.3 \times 10^{21}\ m^{-3}$, $5.2 \times 10^{21}\ m^{-3}$, and $2.1 \times 10^{22}\ m^{-3}$, measured hole mobilities were $6.2 \times 10^{-4}$, $1.34 \times 10^{-4}$, and $1.85 \times 10^{-5}\ cm^2\ V^{-1}\ s^{-1}$, and electron mobilities were $8.2 \times 10^{-4}$, $1.0 \times 10^{-4}$, and $1.0 \times 10^{-5}\ cm^2\ V^{-1}\ s^{-1}$.

As a step towards quantifying recombination rates, we evaluated the agreement between experimental results and simulations with regards to the intensity dependence of $V_{oc}$. In case of Langevin recombination of free carriers being the only loss mechanism, it has been shown that the $V_{oc}$ is given by[15]

$$V_{OC} = \frac{E_{gap}}{q} - \frac{kT}{q} \ln\left[\frac{(1-P)\gamma N_c^2}{PG}\right], \tag{3}$$

where $E_{gap}$ is the energy difference between the HOMO of the electron donor and the LUMO of the electron acceptor, $q$ is electronic charge, $k$ is the Boltzmann constant, $T$ is the temperature, $P$ is the probability of exciton dissociation, $\gamma$ is the recombination constant, $N_c$ is the density of states in the conduction band, and $G$ is the exciton generation rate. Since $G$ is proportional to light intensity, Eq. (3) relates $V_{oc}$ to light intensity; slope ($S$) of $V_{oc}$ versus the logarithm of light intensity being equal to $kT/q$. This has been experimentally verified on various PPV:fullerene devices.[15] However, for devices A, B, and C, the experimental data showed a steeper dependence of $V_{oc}$ on the light intensity with $S = 1.1$, 1.4, and 1.9 times $kT/q$, respectively, whereas the $V_{oc}$ simulated using the aforementioned device model had the expected $kT/q$ slope (Fig. 1). A slope of $1.5(kT/q)$ has been reported for all-polymer solar cells with electron traps in the acceptor phase,[8] and this deviation was rectified by including SRH recombination ($R_{SRH}$) at the donor-acceptor interface in the device model developed for BHJ OPVs.[8,13] The trap-assisted SRH recombination competes with Langevin recombination, therefore the aforementioned slope $S$ increases with the strength of the SRH recombination. At the outset, we did not include the trap-assisted recombination in the device model, because in the earlier studies on P3HT:PCBM OPVs, trap densities were

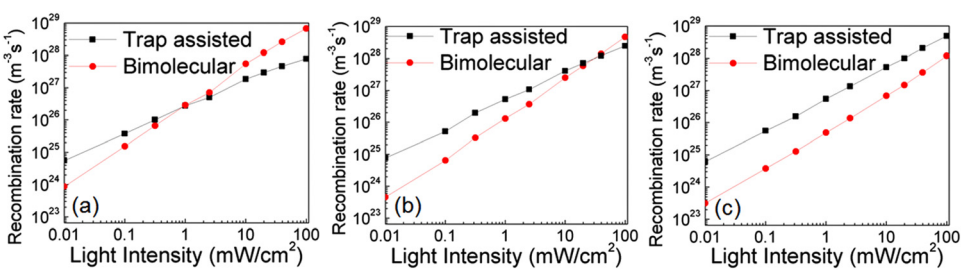


FIG. 2. (Color online) Rate of trap-assisted SRH recombination (squares) and of Langevin recombination (circles) at open circuit condition as a function of light intensity, for devices (a) A, (b) B, and (c) C. The recombination rates were calculated for the parameters used to calculate the current under illumination at 100 mW $cm^{-2}$, with a field dependent generation rate $G$.

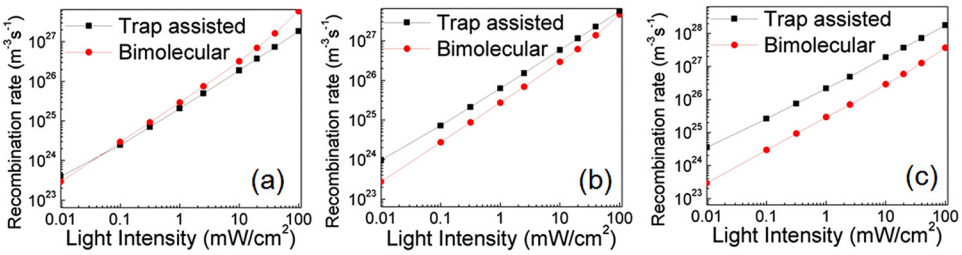


FIG. 3. (Color online) Rate of trap-assisted recombination (squares) and of Langevin (bimolecular) recombination (circles) at short circuit condition as a function of light intensity, for devices (a) A, (b) B, and (c) C.

considered negligible and Langevin recombination was assumed as dominant mechanism.[16] By including SRH recombination in the device model, calculated light-intensity dependence of the $V_{oc}$ (with $R_{SRH}$) became in agreement with the measured values, as shown in Fig. 1. The photocurrent of devices A, B, and C were recalculated after incorporating SRH recombination in the device model (Fig. 1(d)). Good agreement between measured and simulated photocurrent shows that the same framework[13] is able to describe the trap-limited current-voltage characteristics of P3HT:PCBM OPV devices, once the contribution of SRH recombination is included.

To understand and improve the device operation, it is imperative to know which recombination mechanism is responsible for the losses in a solar cell. Fig. 2 illustrates the recombination rates calculated as a function of light intensity for devices A, B, and C at open circuit condition. As shown in Figure 2(a), in device A, the strength of the Langevin recombination is clearly dominant compared to the SRH recombination at 100 mW $cm^{-2}$ (one sun illumination). In device B (Figure 2(b)) also Langevin recombination dominates the SRH recombination, albeit less significantly. This is another reason why the inclusion of SRH recombination was not considered obligatory in earlier models[16] of P3HT:PCBM OPVs and owes to low-enough trap densities in slow grown active-layers. At lower light intensities (<1 and 40 mW $cm^{-2}$ for devices A and B, respectively), trap-assisted recombination is more dominant than Langevin recombination. This is because, with increasing light intensity, leading to an enhanced carrier density in devices, the Langevin recombination becomes quadratically stronger ($\sim np$) and eventually dominates the trap-assisted recombination [$\sim p(n)$]. For fast grown device C, however, which had the strongest dependence of $V_{oc}$ on light intensity and highest defect density ($2.1 \times 10^{22}$ $m^{-3}$), the trap-assisted recombination dominates over the Langevin recombination at all light intensities (Fig. 2(c)), by an order of magnitude.

Fig. 3 illustrates the recombination rates calculated as a function of light intensity for devices A, B, and C at short circuit condition. Similar to the open circuit case, at short circuit condition also, trap-assisted SRH recombination is clearly dominant at all light intensities for device C, and at lower light intensities for devices A and B. Moreover, at one sun condition, owing to the higher SRH recombination, the total recombination rate is 3-4 times higher in device C as compared with device A. This increased amount of SRH recombination in trap-limited device C also leads to the observed reduction of the photocurrent and fill-factor as seen in current-voltage characteristics (Fig. 1).

Above results show that it cannot be generally assumed that trap-assisted recombination is absent in P3HT:PCBM or other OPV cells. It is a strong function of processing conditions. Going from spin-coating the active-layer at 400 rpm for 30 s to spin-coating it at 1000 rpm for 60 s does not appear to be a drastic change to an extent that it will affect which recombination mechanism is the dominant one. But our results clearly show that this processing change significantly increases the defect densities, which leads to domination of trap-assisted recombination over bimolecular recombination, and deteriorates the photocurrent and fill-factor. Thus, it is not surprising that there is not always good reproducibility when different groups use the same processing recipe to fabricate OPVs,[17] as there are processing subtleties that are either not easily identified or typically not explicitly disseminated.

In conclusion, we have shown that for slow grown P3HT:PCBM active layers, bimolecular recombination is the major loss mechanism at one sun condition, and it exceeds the trap-assisted recombination loss by an order of magnitude. However, the trap-assisted recombination dominates at low light intensities. For fast grown active layers with higher trap densities, trap-assisted recombination dominates the bimolecular recombination at all light intensities, and overall recombination rate is 3-4 times higher. Therefore, it becomes imperative to design materials without traps to defect-engineer the OPVs for achieving higher performance. It remains to be seen whether solvent-annealing has an advantage over thermal annealing in terms of reducing traps and trap-assisted recombination and is the subject of our immediate research.

The authors thank Iowa Power Fund and National Science Foundation (Award # 1055930) for supporting this work.

[1]H. Y. Chen, J. H. Hou, S. Q. Zhang, Y. Y. Liang, G. W. Yang, Y. Yang, L. P. Yu, Y. Wu, and G. Li, Nat. Photonics **3**, 649 (2009); Y. Y. Liang, Z. Xu, J. B. Xia, S. T. Tsai, Y. Wu, G. Li, C. Ray, and L. P. Yu, Adv. Mater. **22**, E135 (2010).
[2]G. Li, V. Shrotriya, J. S. Huang, Y. Yao, T. Moriarty, K. Emery, and Y. Yang, Nature Mater. **4**, 864 (2005).
[3]W. L. Ma, C. Y. Yang, X. Gong, K. Lee, and A. J. Heeger, Adv. Funct. Mater. **15**, 1617 (2005).
[4]J. Peet, J. Y. Kim, N. E. Coates, W. L. Ma, D. Moses, A. J. Heeger, and G. C. Bazan, Nature Mater. **6**, 497 (2007); Y. Yao, J. H. Hou, Z. Xu, G. Li, and Y. Yang, Adv. Funct. Mater. **18**, 1783 (2008).
[5]G. Li, Y. Yao, H. Yang, V. Shrotriya, G. Yang, and Y. Yang, Adv. Funct. Mater. **17**, 1636 (2007).
[6]S. Miller, G. Fanchini, Y. Y. Lin, C. Li, C. W. Chen, W. F. Su, and M. Chhowalla, J. Mater. Chem. **18**, 306 (2008).
[7]T. Kirchartz, K. Taretto, and U. Rau, J. Phys. Chem. C **113**, 17958 (2009).

[8]M. M. Mandoc, W. Veurman, L. J. A. Koster, B. de Boer, and P. W. M. Blom, Adv. Funct. Mater. **17**, 2167 (2007).
[9]K. S. Nalwa, R. C. Mahadevapuram, and S. Chaudhary, Appl. Phys. Lett. **98**, 093306 (2011).
[10]P. Langevin, Ann. Chim. Phys. **28**, 433 (1903).
[11]M. M. Mandoc, W. Veurman, L. J. A. Koster, M. M. Koetse, J. Sweelssen, B. de Boer, and P. W. M. Blom, J. Appl. Phys. **101**, 104512 (2007).
[12]R. A. Street and M. Schoendorf, Phys. Rev. B **81**, 205307 (2010).
[13]L. J. A. Koster, E. C. P. Smits, V. D. Mihailetchi, and P. W. M. Blom, Phys. Rev. B **72**, 085205 (2005).
[14]H. K. Kodali and B. Ganapathysubramanian, "Computer simulation of heterogeneous polymer photovoltaic devices," Modell. Simul. Mater. Sci. Eng. (to be published).
[15]L. J. A. Koster, V. D. Mihailetchi, R. Ramaker, and P. W. M. Blom, Appl. Phys. Lett. **86**, 123509 (2005).
[16]A. Pivrikas, G. Juska, A. J. Mozer, M. Scharber, K. Arlauskas, N. S. Sariciftci, H. Stubb, and R. Osterbacka, Phys. Rev. Lett. **94**, 176806 (2005); A. Foertig, A. Baumann, D. Rauh, V. Dyakonov, and C. Deibel, Appl. Phys. Lett. **95**, 052104 (2009).
[17]S. H. Tolbert, B. T. de Villers, C. J. Tassone, and B. J. Schwartz, J. Phys. Chem. C **113**, 18978 (2009).